Effect of Rice Husk Ash Insulation Powder on the Reoxidation Behavior of Molten Steel in Continuous Casting Tundish

TAE SUNG KIM, YONGSUG CHUNG, LAURI HOLAPPA, and JOO HYUN PARK

Rice husk ash (RHA) has been widely used as an insulation powder in steel casting tundish. Its effect on the reoxidation of molten steel in tundish as well as on the corrosion of magnesia refractory was investigated. The reoxidation of the steel, indicated by an oxygen pickup, was progressed by increasing the ratio of RHA to the sum of RHA and carryover ladle slag (*R* ratio) greater than about 0.2. The increase of the silica activity in the slag layer promoted the self-dissociation of SiO_2 from the slag layer into the molten steel, resulting in the silicon and oxygen pickup as the *R* ratio increased. The total number of reoxidation inclusions dramatically increased and the relative fraction of Al_2O_3-rich inclusions increased by increasing the *R* ratio. Hence, the reoxidation of molten steel in tundish might become more serious due to the formation of alumina-rich inclusions as the casting sequence increases. MgO in the refractory directly dissolved into the molten slag layer without forming any intermediate compound layer (*e.g.*, spinel), which is a completely different situation from the general slag-refractory interfacial reaction. A flow was possibly induced by the bursting of gas bubbles at the ash-slag (-refractory) interface, since the silica in the RHA powder continuously dissolved into the molten slag pool. Thus, the RHA insulation powder has a negative effect on the corrosion of MgO refractory.

DOI: 10.1007/s11663-017-0971-3

I. INTRODUCTION

IT is important to improve the cleanliness of molten steel in tundish for manufacturing high-quality steel products. The tundish has an important role in cleaning the molten steel by coagulation and floating up of nonmetallic inclusions in conjunction with distributing the molten steel to single or multiple casting strands.[1] However, the contamination of molten steel occurs in tundish by various factors, including the entrapment of carryover ladle slag, reaction with tundish flux, degradation of refractory, reaction with ladle well packing material, oxidation of molten steel by residual slag and metal, and oxidation of molten steel by air.[1–4] The changes in inclusion characteristics in the tundish can even influence the submerged nozzle clogging.

The reoxidation behavior of molten steel in the tundish can be divided into an initial teeming stage at the beginning of the casting or transition period and a stable teeming stage. The oxidation by air occurs at the initial teeming stage, because the molten steel becomes exposed to ambient as it is devoid of tundish flux by the turbulent flow.[5–8] The effect of the oxidation by air, however, is negligible to the reoxidation of molten steel under dilute oxygen condition, *i.e.*, $p(O_2) = 7.4 \times 10^{-4}$ atm, which was reported by Higuchi *et al.*[9] Thus, it can be assumed that the reaction between molten steel and tundish flux is a predominant factor affecting the reoxidation phenomena in tundish when the flow of the air into the tundish was prevented by Ar protection.

At the stable teeming stage, the molten steel in tundish would react with tundish flux; hence, tundish flux needs less amounts of reducible oxide, such as iron oxide, manganese oxide, or silica, for preventing reoxidation. Kuchar and Holappa mentioned that double layer tundish slag, which consists of a solid powder layer at the upper part and a liquid slag layer at the reaction zone, in the vicinity of molten steel could prevent the steel in the tundish from both heat loss and reoxidation, as shown in Figure 1.[6] However, rice husk ash (RHA), which contains up to 90 pct silica, is commonly used for tundish flux to provide excellent protection from heat loss.[10] Thus, the reoxidation of molten steel should be reconsidered for a long casting sequence because of continuous dissolution of SiO_2 from the RHA powder layer to the molten slag pool.

Because the dissolution of SiO_2 from RHA to the molten slag increases silica activity in the slag, understanding the interfacial reaction between Al-containing steel and silicate slags is necessary to reveal the reoxidation behavior of molten steel in tundish. Several authors have investigated the interfacial reactions with regard to the kinetic analysis for the reoxidation of Al in the molten metal.[11–14] High content of silica in tundish

TAE SUNG KIM and JOO HYUN PARK are with the Department of Materials Engineering, Hanyang University, Ansan 15588, Korea. Contact email: basicity@hanyang.ac.kr YONGSUG CHUNG is with the Department of Advanced Materials Engineering, Korea Polytechnic University, Siheung 15073, Korea. LAURI HOLAPPA is with the School of Chemical Technology, Aalto University, Espoo 00076, Finland.

Manuscript submitted September 1, 2016.
Article published online April 6, 2017.

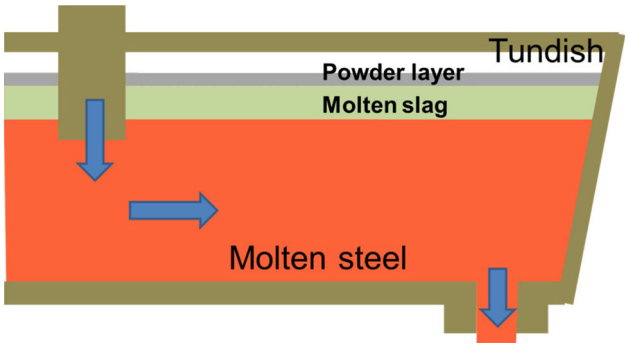

Fig. 1—Schematic diagram of the tundish, in which the RHA powder covers the molten slag layer contacted with molten steel.

flux could cause self-dissociation of SiO_2 into Si and O at the slag-metal interface; hence, soluble oxygen is supersaturated in the molten steel. The supersaturated oxygen results in the contamination of Al-containing steel by formation of Al_2O_3 inclusions.[15–17]

In addition, one of the important phenomena that should be considered in tundish is the corrosion of magnesia refractory lining from the viewpoint of lifetime of the refractory. In general, the formation of spinel layer at the refractory hot face can retard the corrosion of refractory, because the component in the refractory indirectly dissolves into the molten slag by formation of a spinel layer.[18–20] In particular, Chen *et al.*[19] reported that significant corrosion of MgO refractory was observed in contact with alumina-free CaO-SiO_2-FeO_x-MgO slag at 1803 K (1530 °C), while the formation of spinel layer at the slag-refractory interface in the CaO-SiO_2-Al_2O_3-FeO_x-MgO slag retarded the dissolution of MgO refractory.

Therefore, the input of large amounts of RHA to tundish may cause not only contamination of molten steel but also severe corrosion of magnesia refractory lining during long sequence continuous casting. Even though the RHA has been widely used in industry for many years, the number of quantitative evaluations for the reoxidation behavior of molten steel by the interfacial reaction between tundish slag and molten steel is quite low. Therefore, in the present study, we investigated how the RHA affects the reoxidation of molten steel in tundish as well as the corrosion of magnesia refractory.

II. EXPERIMENTAL

Reagent grade SiO_2, Al_2O_3, and CaF_2 were used in the present experiments. CaO and MgO were obtained from reagent grade $CaCO_3$ and $MgCO_3$, which were calcined at 1273 K (1000 °C) for 10 hours. The powders were weighed and mixed for 1 hour to obtain homogeneous mixtures. The mixtures were melted in a graphite crucible at 1873 K (1600 °C) in order to prepare the carryover ladle slag. The compositions of the simulated ladle slag and the commercial RHA powder used in the present experiments are listed in Table I.

A schematic diagram of the experimental apparatus is shown in Figure 2. Electrolytic iron was contained in a fused magnesia crucible (99.9 pct purity, 60 × 50 × 130 mm) with reagent grades carbon and metal silicon for obtaining the required steel composition. The magnesia crucible containing the Fe-0.2C-0.1Si (mass pct) steel (500 g) was set in a high-frequency induction furnace combined with a graphite heating element. The quartz reaction chamber was initially evacuated using a mechanical rotary pump and then filled with the Ar-3 pct H_2 gas mixture. The steel contained in a magnesia crucible was heated using induction heat under Ar-H_2 gas atmosphere. In order to improve gas purity, the Ar-H_2 gas mixture was passed through the magnesium turnings heated to 723 K (450 °C). A B-type thermocouple for measuring temperature of the system was positioned on the inner wall of the crucible.

The Fe-C-Si steel was heated to 1823 K (1550 °C), and then the Fe-16 pct Al alloy (0.94 g) was added through the quartz tube (14 × 12 × 500 mm) under Ar-H_2 atmosphere. The initial steel sample was taken using a quartz tube (8 × 6 × 500 mm) 15 minutes after the Fe-16 pct Al was added. As soon as the initial sampling was completed, the commercial grade Ar gas (99.9 pct purity) was injected to the quartz reaction chamber without passing the magnesium turnings furnace and the Ar-3 pct H_2 flow was closed.

The premelted ladle slag was first poured onto the molten steel, and then the RHA powder was added on the ladle slag for simulating the actual condition in continuous casting tundish. The total amount of RHA and ladle slag was 50 g. The experiments were carried out varying the mass ratio of RHA to the sum of RHA and ladle slag (=[RHA]/[RHA + SLAG] = *R* ratio = 0.14, 0.26, 0.38, and 1.0). A steel sample was taken at predetermined times from the start of the experiment, equal to 5, 10, 30, and 60 minutes, and it was rapidly quenched in water. A slag sample was also taken at the predetermined times of 30 and 60 minutes and was rapidly quenched in an Ar gas stream. The steel and slag samples were about 10 and 1 g, respectively, per each sampling.

The total oxygen and nitrogen contents in the steel samples were analyzed by the combustion analysis method. Also, the total amounts of Si and Al in the steel were analyzed by inductively coupled plasma–atomic emission spectroscopy (ICP-AES, iCAP6500, Thermo Scientific, Waltham, MA). The characterization of inclusions, *i.e.*, number density, morphology, and composition, in the steel samples taken at 5 minutes was performed using field-emission–scanning electron microscopy (FE-SEM) with an energy-dispersive X-ray spectroscope (EDS, MIRA 3, TESCAN Ltd., Czech). The inclusions in the sample were observed using the automated inclusion analysis system with the following settings: magnification 500 times, 0.5-μm pixel size, and 1-μm limit diameter for inclusion detection in the 2 mm × 2 mm area.

Separate experiments were carried out in order to observe the high-temperature behavior of RHA powder, for example, the evolution of gas bubbles within the

Table I. Initial Composition of the Simulated Carryover Ladle Slag and Commercial RHA Powder Used in the Present Experiments (Mass Pct)

Type	CaO	Al_2O_3	SiO_2	MgO	CaF_2	C
Ladle slag	45	35	10	5	5	—
RHA	4	7	73	1	—	15

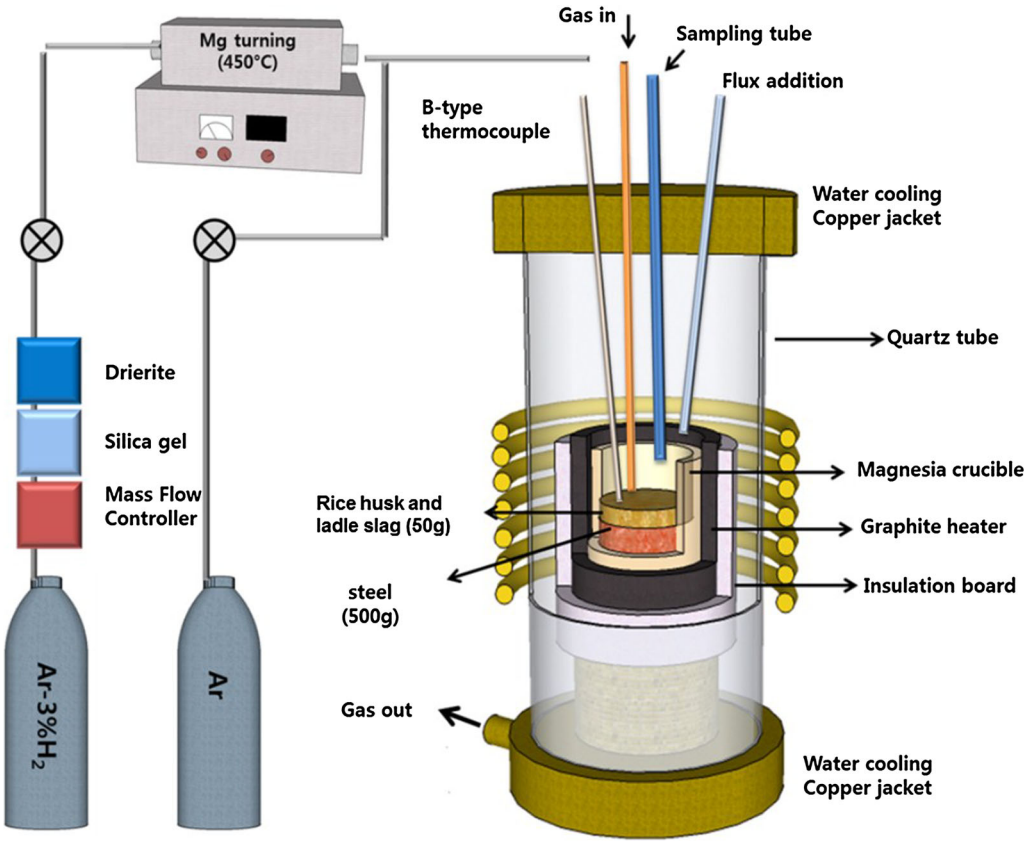

Fig. 2—Schematic diagram of the experimental apparatus.

RHA powder due to the internal chemical reaction between SiO_2 and solid carbon, which affected the ash-slag-refractory reaction in the tundish. Commercial RHA powder was grinded and sieved as under 100-μm size. The sieved RHA was placed in a metallic mold and pressed to produce a disc-shaped pellet (diameter: 8 mm, height: 5 mm). The pellet was heated to 1793 K (1520 °C) under the commercial grade Ar gas (99.9 pct purity), after which it was positioned in the center of a horizontal furnace. Images of the changes of the RHA pellet were recorded using a CCD camera.

III. RESULTS AND DISCUSSION

A. *Reoxidation of Al-Killed Steel by Atmosphere*

The total oxygen and nitrogen contents in the Al-killed steel with different R ratios are shown in Figure 3 as a function of reaction time at 1823 K (1550 °C). The initial content of oxygen in the Al-killed steel was about 11(±3) ppm. In Figure 3(a), the oxygen content in the steel was rarely changed through the entire experiment when the relatively small amounts of RHA (R ratio = 0.14) were added. However, the oxidation of the steel augmented by increasing the RHA (R ratio = 0.26, 0.38, and 1.0), which means that oxygen pickup (ΔO) significantly occurred within the first 10 minutes for an R ratio greater than about 0.26.

The oxygen content decreased after 10 minutes, which originated from the flotation removal of the inclusions. Also, the oxygen content was higher as the R ratio increased, because the dissolution rate of inclusion was decreased by the highly viscous slag. Although the influence of the physicochemical properties of the slag on the inclusion removal rate is an important topic, the removal process of the inclusions is beyond the scope of the present study but is fully discussed in our previous

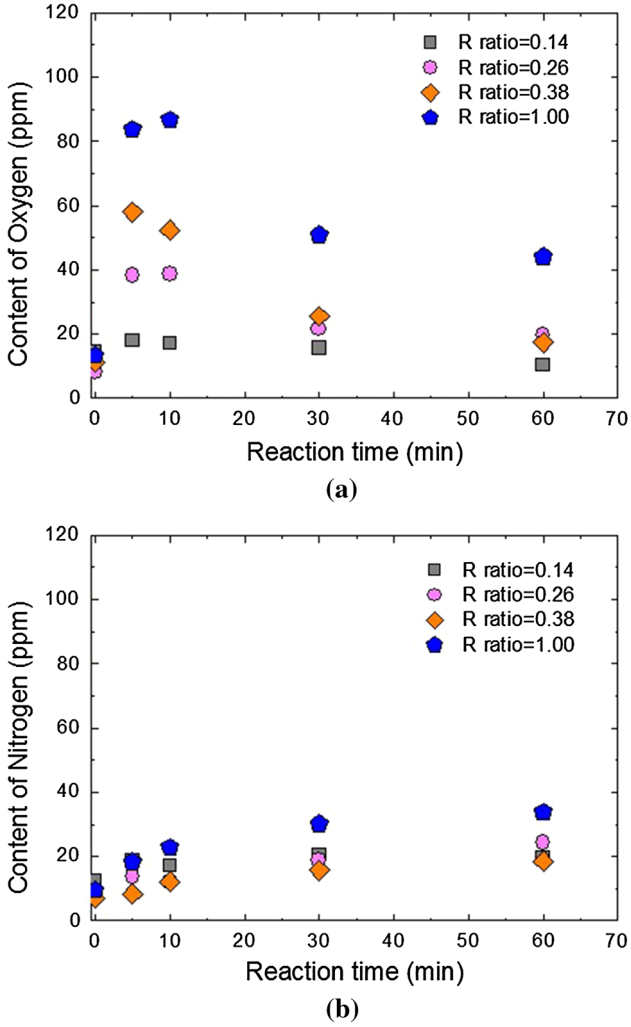

Fig. 3—Content of (*a*) total oxygen and (*b*) total nitrogen in the steel melt with reaction time.

article.[21] Therefore, the initial oxygen pickup and the related phenomena due to the reoxidation of molten steel within 10 minutes are considered in the present study. The characterization of inclusions by their morphology, chemistry, and number density is systematically discussed in Section III–B–4.

Tanaka *et al.*[5] reported that oxygen remaining in tundish atmosphere was the most important factor affecting the contamination of molten steel during casting compared to slag-metal reaction when the oxygen partial pressure in tundish atmosphere was about $p(O_2) = 0.05$ atm. On the other hand, Higuchi *et al.*[9] investigated the reoxidation of molten steel by tundish slag under condition of $p(O_2) = 7.4 \times 10^{-4}$ atm. Since the oxygen content calculated from both the nitrogen partial pressure and the flow rate of Ar gas was too low to reoxidize the steel in tundish and the increase of nitrogen content in the steel was not observed, they concluded that the effect of air on the reoxidation of molten steel in tundish was negligible.[9] Thus, the slag-metal reaction was the significant factor affecting the reoxidation when the molten steel was fully covered by the slag layer at steady state.

In Figure 3(b), the nitrogen pickup (ΔN) to molten steel was not so significant, *i.e.*, $\Delta N = 15(\pm 3)$ ppm during the entire experiment (60 minutes) irrespective of the R ratio. Since the source of nitrogen is only the impurity gaseous species in a commercial grade (99.9 pct, unpurified) Ar gas, a degree of nitrogen pickup indicates a degree of reoxidation by gaseous atmosphere. In the present study, therefore, it can be considered that the gaseous reoxidation of molten steel was not so significant in the commercial purity Ar atmosphere and the slag-metal reaction was the main cause for reoxidation of molten steel.

B. *Reoxidation of Al-Killed Steel by Slag-Metal Reaction*

1. *Change of Al and Si content in steel melt*

The change of Al and Si concentration in the steel is shown in Figure 4 as a function of reaction time and R ratio at 1823 K (1550 °C). The initial contents of Al and Si were about 0.03 and 0.1 mass pct, respectively. The solid lines in Figure 4 represent the calculated results based on the kinetic analysis, which will be discussed in Section III–B–2. As soon as the ladle slag and the RHA were added on molten steel, the oxidation of Al progressed within 10 minutes, as shown in Figure 4(a). The reoxidation rate of Al was fast regardless of the RHA content. The content of Si in the steel increased, because the SiO_2 in the slag was reduced by the Al in the steel within 10 minutes, as shown in Figure 4(b). The Si pickup was more serious as higher amounts of RHA were added. There were some scatters between measured and calculated Si contents at the early stage of the reaction because of inhomogeneity of the interface between the molten steel and RHA layer (*i.e.*, not fully molten at the interface) when only a single RHA was used.

The major reoxidation reaction of the steel would take place at the slag-metal interface. The results in Figure 4 suggest that the reduction of SiO_2 by Al in molten steel occurs by the following reaction:

$$4[Al] + 3(SiO_2) = 2(Al_2O_3) + 3[Si] \qquad [1]$$

The reduction rate of SiO_2 from the slag increased by the addition of RHA, while the oxidation rate of Al in the steel was not critically dependent on the R ratio. Furthermore, the content of Si in molten steel continuously increased during the entire experimental period, *viz.* 60 minutes. The increase of SiO_2 content in the slag by addition of RHA might affect the reduction of SiO_2 more seriously compared to the oxidation of Al.

Holappa and co-workers[6–8] investigated the reoxidation behavior of molten steel in tundish by employing the actual steel plant data. In these studies, the RHA was used for preventing the molten steel from the heat loss. The Si pickup from slag into molten steel was clearly observed in conjunction with the loss of Al content. These phenomena were especially serious at the

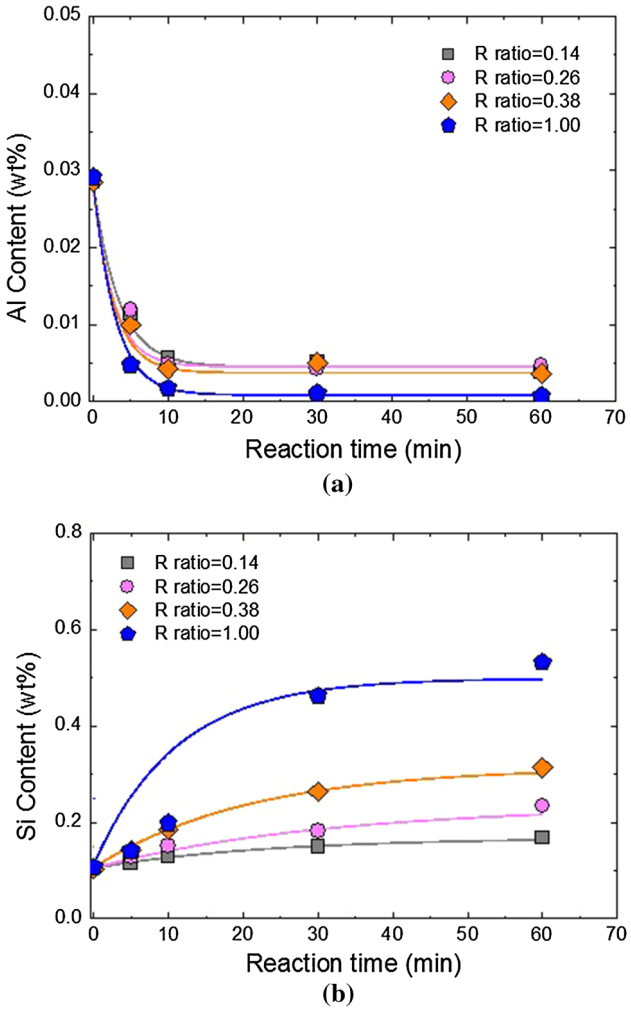

Fig. 4—Changes in concentration of (*a*) Al and (*b*) Si in the steel as a function of reaction time at 1823 K (1550 °C).

beginning of the casting or ladle transition period, since the steel was not fully protected by the tundish cover powder. Once the steel flow in tundish was in a stationary state, the steel was fully covered by the double layer, which consisted of tundish cover powder and carryover ladle slag. Because the basicity of the carryover ladle slag was relatively high, the potential reduction of SiO_2 in tundish cover powder, *e.g.*, RHA, would diminish by introduction of the carryover ladle slag into the tundish.[6]

However, it should be considered that the dissolution of SiO_2 from the RHA to the molten slag layer takes place at the double layer interface during the stationary state in tundish; hence, the SiO_2 content in the molten slag increases during casting sequence. The increased SiO_2 content in the molten slag could cause the reoxidation of the steel by the slag-metal reaction given in Eq. [1]. Therefore, the dissolution rate of SiO_2 from the RHA to the slag phase is one of the important factors affecting the reoxidation of molten steel.

Feichtinger *et al.*[22] investigated the dissolution rate of pure silica into the $CaO\text{-}SiO_2\text{-}Al_2O_3$ slag with relatively high silica (37 to 55 mass pct) and low alumina (10 to 26 mass pct) combinations. They concluded that the dissolution rate of silica was strongly dependent on the viscosity of the slags; *viz*. the lower the viscosity of molten slags was, the higher the observed dissolution rate of silica into the molten slags. The dissolution rate (=shrinking rate of spherical silica particle in Reference 22) was about 11.0×10^{-6} m/s when the viscosity of molten slag was about 0.5 Pa·s at 1723 K (1450 °C). Because the viscosity of the simulated carryover ladle slag, which was directly measured by the rotating cylinder method by the present authors in a previous study,[23] in the present experiment is about 0.1 to 0.2 Pa·s at 1823 K (1550 °C), it can be reasonably assumed that the dissolution transfer rate of SiO_2 from RHA to molten slag layer is considerably faster in the present experimental conditions compared to the results of Feichtinger *et al.*[22]

2. *Interfacial reaction kinetics between molten steel and slag layer*

For the reoxidation of Fe-Al melt by the $CaO\text{-}Al_2O_3\text{-}SiO_2$(-FeO,MnO) slags, Sun and Mori concluded that the slag-metal reaction given in Eq. [1] in the low SiO_2 region was controlled by the chemical reaction, *i.e.*, the dissociation of SiO_2 into *Si* and *O* at the metal-slag interface, because the oxidation rate of Al by the SiO_2-containing slags was lower than that by the FeO(or MnO)-containing slags.[11] On the other hand, Rhamdhani *et al.*[12] and Kang *et al.*[13] concluded that the slag-metal reaction was controlled by the mass transfer of Al in the metal phase.

The mixed (metal + slag phase mass transfer) control for Eq. [1] was proposed by Park *et al.*[14] That is, the reaction rate of Eq. [1] is controlled not only by the mass transfer of Al in the metal phase but also by the mass transfer of SiO_2 in the slag phase when the SiO_2 concentration in the slag is low. They reported that a decrease in SiO_2 content by the reaction (Eq. [1]) causes lack of SiO_2 at the interfacial boundary layer when the initial SiO_2 content is quite low. The slag-metal reaction is controlled by mass transfer of Al in the metal phase when the concentration of Al in the metal is low.

The present experiments were carried out under conditions of low Al content in the steel, *i.e.*, about 0.03 mass pct, and of high SiO_2 content in the slag layer, *i.e.*, continuous dissolution and transfer of SiO_2 from the rice husk powder layer to molten slag pool. Therefore, it is reasonable to assume that the slag-metal reaction given in Eq. [1] is controlled by the mass transfer of Al in the metal phase. Based on the preceding discussions, the interfacial reaction kinetics can be evaluated, as discussed in a previous study.[24]

The net flux of Al (J_{Al}) in the molten steel as a function of reaction time can be written as

$$J_{Al} = k_{Al}\left(C^{b}_{m,Al} - C^{i}_{m,Al}\right) \qquad [2]$$

$$J_{Al} = -\frac{dC^{b}_{Al}}{dt}\frac{V_m}{A} = k_{Al}\left(C^{b}_{m,Al} - L_{Al}C^{b}_{s,Al}\right) \qquad [3]$$

$$L_{Al} = \frac{C^{i}_{m,Al}}{C^{i}_{s,Al}} = \frac{C^{eq}_{m,Al}}{C^{eq}_{s,Al}} \quad [4]$$

where k_{Al} is the mass-transfer coefficient of Al in the metal phase (m/s); C_{Al} is the molar content of Al (mol/m^3); V is the volume of metal and slag (m^3); A is the reaction area between the slag and the metal (m^2), which is assumed as the inner cross-sectional area of the crucible; and L_{Al} is the distribution ratio of Al between metal and slag. The superscripts b, i, and eq represent bulk, interface, and equilibrium, respectively, and the subscripts s and m represent slag and metal phases, respectively. The following equation is acquired by integrating Eq. [3].

$$-\ln \frac{[\text{pct Al}]_t - [\text{pct Al}]_e}{[\text{pct Al}]_0 - [\text{pct Al}]_e} = k_{Al} \frac{A}{V_m} \left(\frac{[\text{pct Al}]_0}{[\text{pct Al}]_0 - [\text{pct Al}]_e} \right) t \quad [5]$$

where t is the reaction time (s), $[\text{pct Al}]_t$ is the concentration of Al in the steel at reaction time t, $[\text{pct Al}]_0$ is the initial concentration of Al in the steel, and $[\text{pct Al}]_e$ is the equilibrium concentration of Al in the steel. The mass-transfer coefficient of Al in the metal phase, k_{Al}, can be calculated from Eq. [5] to be 1.5 to 2.0×10^{-4} m/s at 1823 K (1550 °C) in the present study.

Rhamdhani *et al.*[12] and Kang *et al.*[13] claimed that the mass transfer of Al in liquid steel is the rate-determining step when the content of Al in molten steel is lower than about 4 mass pct. Rhamdhani *et al.* suggested $k_{Al} = 1.7 \times 10^{-6}$ m/s at 1923 K (1650 °C), while Kang *et al.* reported $k_{Al} = 0.9$ to 1.2×10^{-4} m/s at 1773 K (1500 °C), a value that is in accordance with the value 1.5 to 2.0×10^{-4} m/s at 1823 K (1550 °C) of the present study. Rhamdhani *et al.*[12] carried out the experiments by injecting metal droplets into molten slag, and the weight of the slag was larger than that of the metal. Because a significant emulsification was observed under their experimental conditions, they counted the surface area of all steel droplets emulsified in the slag when they estimated the mass-transfer coefficient. However, Kang *et al.*[13] carried out the experiments by pouring premelted slag on the molten steel, in which condition the strong metal emulsification was not observed. Thus, they assumed that the interfacial reaction area is a cross section of the crucible containing the molten steel and slag. As the present study was carried out in a similar condition, it is reasonable that the present results are comparable to those of Kang *et al.*[13]

3. *Interfacial reaction mechanism between molten steel and slag layer*

It is noteworthy that the reoxidation rate of Al in the steel melt did not significantly change due to the ratio of RHA to ladle slag, as shown in Figure 4(a). Even the Al content remained almost constant after 10 minutes. On the other hand, the reduction rate of SiO_2 from the slag increased by the addition of RHA, as shown in Figure 4(b), and the reaction did not cease but continued after 10 minutes. Therefore, the mass balance relationship between the consumption of Al and the production of Si at 10 minutes was calculated based on Eq. [1], which is shown in Figure 5 for different R ratios. The Si content produced was much larger than that expected from the reaction stoichiometry of Eq. [1], and the scatter increased with increasing R ratio, which means that Si in the steel melt was generated by another reaction apart from Eq. [1], *viz.* self-dissociation of SiO_2.

Bessho *et al.*[1] reported that the molten steel in tundish is contaminated by Si when the silica activity, a_{SiO_2}, in tundish flux is greater than about 0.12, while high basicity flux ($a_{SiO_2} < 0.008$) does not cause the Si pickup. Park *et al.*[15] reported that the self-dissociation of SiO_2 occurs from the SiO_2-rich tundish slag (*i.e.*, 14CaO-35Al_2O_3-10MgO-41SiO_2, mass pct), resulting in supersaturation of oxygen in the steel and oxidation of Al and Ti. Chung[16] and Tanaka *et al.*[17] also presented

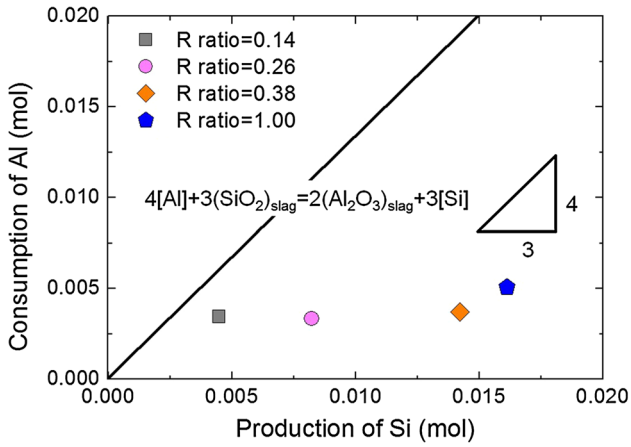

Fig. 5—Mass balance between production of Si and consumption of Al in the steel.

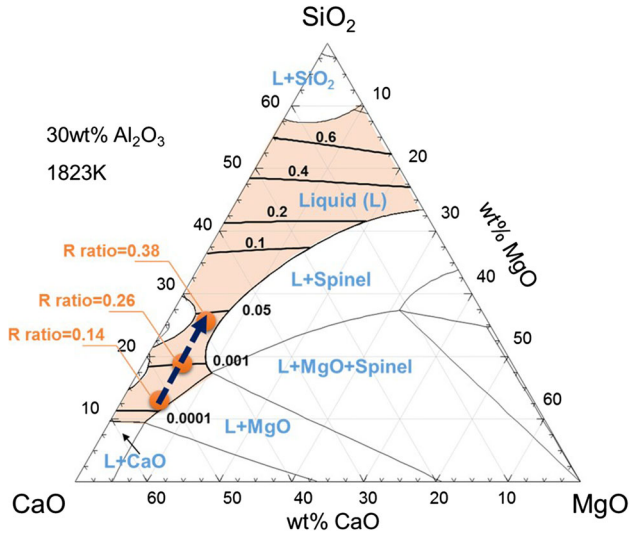

Fig. 6—Iso-activity contours of SiO_2 in the CaO-SiO_2-MgO-30 pct Al_2O_3 system calculated by FACTSAGE™ 7.0 at 1823 K (1550 °C). Black arrow shows slag compositions at various R ratios.

that Si and O dissociate from SiO_2 at the slag-metal interface transfer into the Fe-Al alloy, and O further reacts, forming Al_2O_3 clusters in the alloys. Thus, the silica activity in the slag is a key factor affecting the Si pickup into the molten steel in the tundish.

The changes in the composition of slag with reaction time are shown in the CaO-SiO_2-MgO-30 pct Al_2O_3 phase diagram at 1823 K (1550 °C), as shown in Figure 6. The quaternary phase diagram and the iso-activity contours were calculated using a commercial thermochemical simulation program, FACTSAGE™ 7.0 with "FTOXID" database. This package has been successfully used for the prediction of thermochemical properties of steel-slag-refractory-gas equilibria at high temperatures.[25–29]

It was significantly difficult to take slag samples at the initial stage of the slag-metal reaction, *e.g.*, 5 and 10 minutes, because a solid (crispy) rice husk powder layer covered the ladle slag. Hence, the activity of SiO_2 in the slag layer was considered from the experimental data obtained at 30 and 60 minutes, which are listed in Table II. The slag compositions located in the liquid–solid coexisting area due to the corrosion of the refractory phase, which will be discussed in Section III–C. However, the liquid fraction was over 0.80 at all *R* ratios, and the silica activity in the liquid slag phase could be qualitatively inferred from the iso - a_{SiO_2} contours given in Figure 6, in which the activity of SiO_2 in the slag layer increases from 3.5×10^{-4} to 3.4×10^{-3} when the *R* ratio increases from 0.14 to 0.38.

Table II. Compositional Changes of the Slag with *R* Ratio (Mass Pct)

R Ratio	Reaction Time (Min)	CaO	Al_2O_3	SiO_2	MgO	CaF_2	Liquid Fraction	Activity of SiO_2 in Liquid Slag
0.14	30	42.2	30.5	16.9	8.2	2.2	1.00	3.5×10^{-4}
	60	42.1	31.0	13.0	11.6	2.2	0.98	3.5×10^{-4}
0.26	30	38.2	28.4	18.2	13.3	1.9	0.92	7.1×10^{-4}
	60	36.7	28.1	17.6	15.8	1.9	0.89	7.1×10^{-4}
0.38	30	32.6	25.4	25.6	14.8	1.6	0.88	3.4×10^{-3}
	60	31.9	25.9	20.4	20.3	1.6	0.80	1.4×10^{-3}

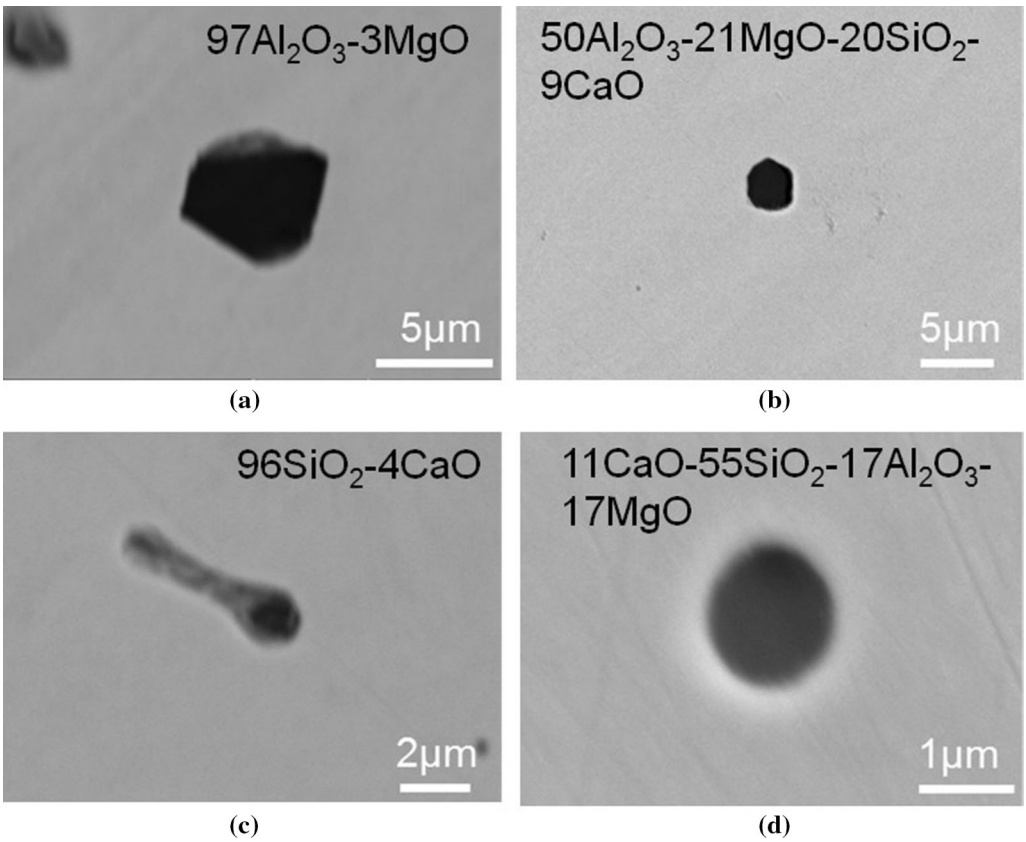

Fig. 7—Typical SEM micrograph of the inclusions in steel sample at 5 min: (*a*) Al_2O_3 rich, (*b*) Spinel type, (*c*) SiO_2 rich, and (*d*) liquid inclusion (numbers represent mass pct).

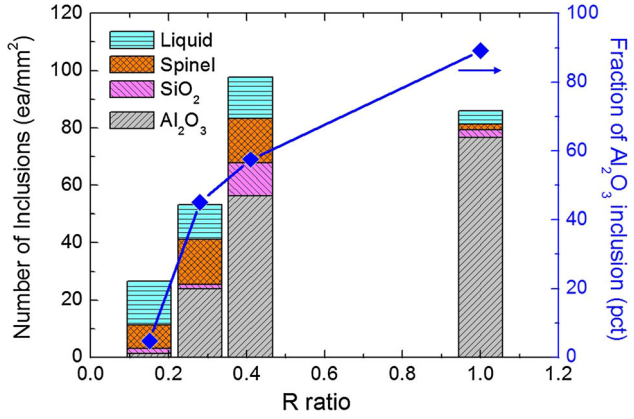

Fig. 8—Number of various types of inclusions per unit area and the relative fraction of Al_2O_3-rich inclusion at 5 min as a function of *R* ratio.

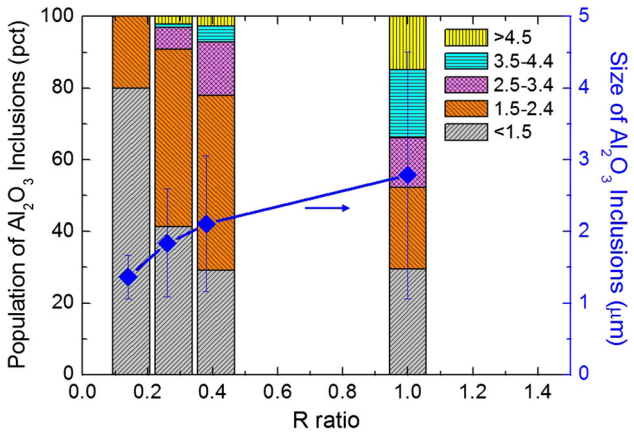

Fig. 9—Size distribution and the average size of Al_2O_3-rich inclusion at 5 min as a function of *R* ratio.

4. *Effect of rice husk on the formation of inclusions via reoxidation in molten steel*

The increase of the silica activity in the slag layer with *R* ratio promotes the self-dissociation of SiO_2 from the slag layer into the molten steel (*i.e.*, $SiO_2 = Si + 2O$), which causes silicon and oxygen pickup. The inclusions in the steel sample at 5 minutes were observed using SEM, and typical SEM images for the inclusions are illustrated in Figure 7, in which four types of inclusions are given, *viz.* Al_2O_3 rich ($Al_2O_3 > 90$ mass pct, Figure 7(a)), spinel type (mainly $MgAl_2O_4$, Figure 7(b)), SiO_2 rich ($SiO_2 > 90$ mass pct, Figure 7(c)), and liquid (falling in liquid area in the MgO-Al_2O_3-SiO_2-CaO phase diagram at 1823 K (1550 °C), Figure 7(d)).

The total number of inclusions per unit area in the steel samples (at 5 minutes) dramatically increased as the *R* ratio increased from 0.14 to 0.38, as shown in Figure 8. The number of inclusions in the steel samples when *R* ratio = 1.0 (*i.e.*, only RHA was used) was slightly lower than that found for *R* ratio = 0.38 but was not so different from it. However, it is noticeable that the relative fraction of Al_2O_3-rich inclusions increased from about 60 to 90 pct as the *R* ratio

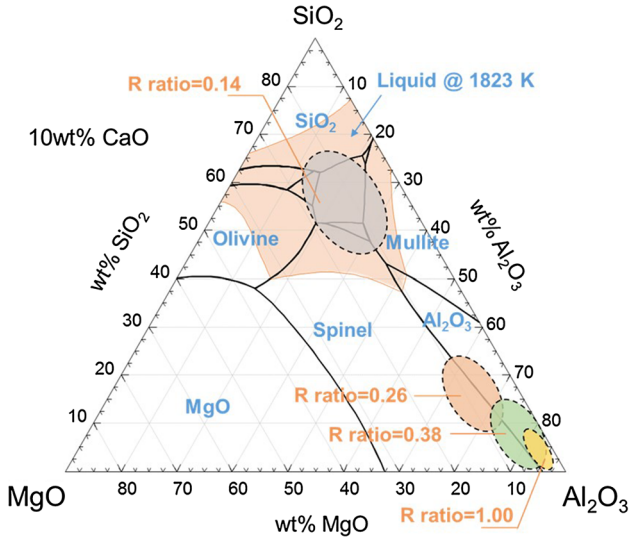

Fig. 10—Composition of the inclusions at different *R* ratios.

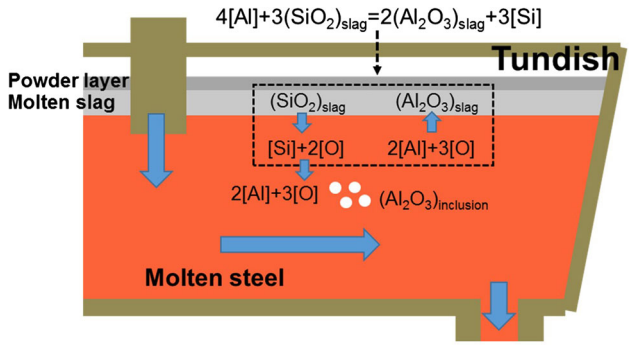

Fig. 11—Schematic diagram for the reoxidation phenomena originated from the slag-metal interfacial reactions in tundish.

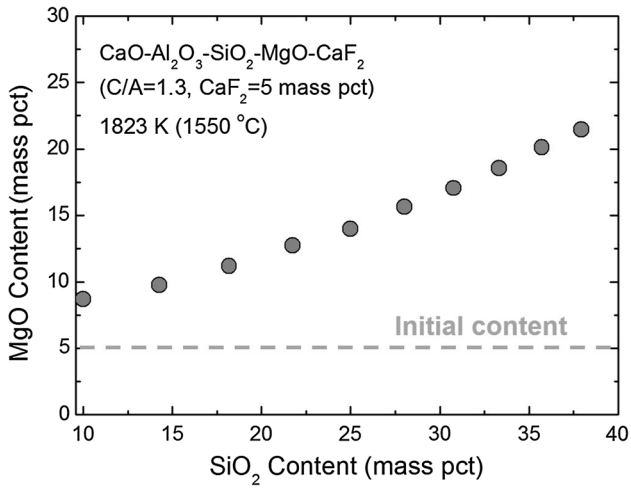

Fig. 12—Solubility limit of MgO in the slag phase as a function of SiO_2 content at 1823 K (1550 °C).

increased from 0.38 to 1.0, which was mainly due to a significant reoxidation.

The size distribution and average diameter of Al_2O_3-rich inclusions in the 5-minute steel samples are shown in Figure 9. When the *R* ratio was 0.14, the observed inclusions were smaller than 2.5 μm. However, the relative abundance of fine (smaller than 1.5 μm) Al_2O_3 inclusions sharply decreased, while the proportion of inclusions larger than 2.5 μm increased when the *R* ratio was greater than 0.26. Specifically, the inclusions larger than 3.5 μm were about 35 pct when only a RHA was used (*i.e.*, *R* ratio = 1.0). Therefore, the average size of the inclusions increased by increasing the *R* ratio, which originated from a significant reoxidation of molten steel due to large amounts of RHA.

The spinel-type inclusions were formed by the reaction between Al_2O_3 inclusions and Mg originated from slag phase. The related reactions are given as follows.[30]

$$3(MgO)_{slag} + 2[Al] = 3[Mg] + (Al_2O_3)_{slag} \quad [6]$$

$$(Al_2O_3)_{inclusion} + [Mg] + [O] = MgAl_2O_4(s) \quad [7]$$

The number of spinel-type inclusions increased as the *R* ratio increased, which was mainly due to an increase in the MgO activity in the slag caused by corrosion of the MgO refractory. Further discussion about the corrosion phenomena of the refractory into the slag is presented in Section III–C.

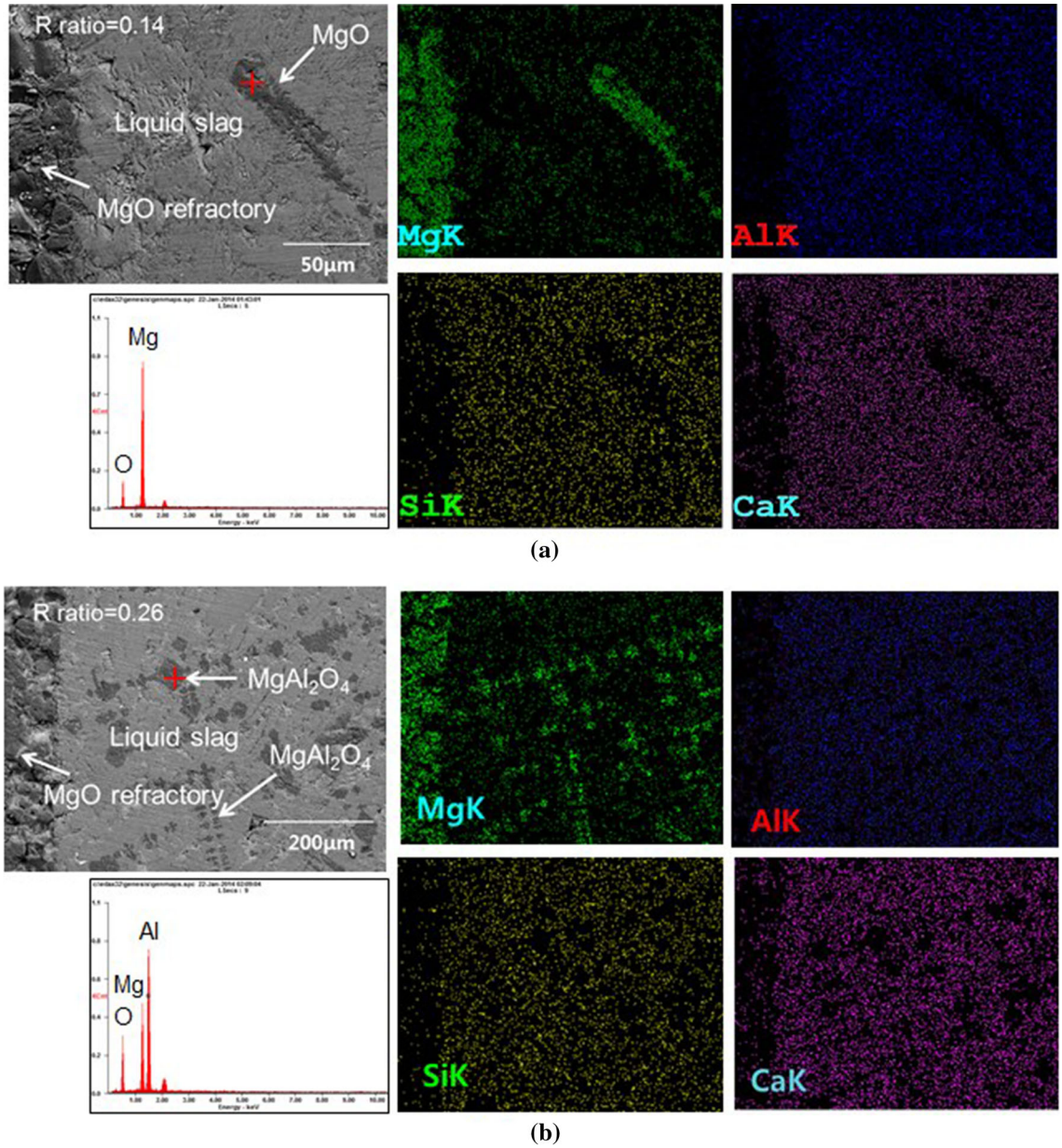

Fig. 13—Backscattered electron image and the element mapping results for the slag-refractory interfacial area at (*a*) *R* ratio = 0.14 and (*b*) *R* ratio = 0.26.

The mean composition ranges of inclusions with R ratios of 0.14, 0.26, 0.38, and 1.0 are shown in the MgO-SiO_2-Al_2O_3-10 pct CaO phase diagram at 1823 K (1550 °C) in Figure 10. The composition of the inclusions at R ratio = 0.14 mainly located in the liquid region with small amounts of SiO_2-rich particles. When the R ratio increased to 0.26, the Al_2O_3 content in the inclusions sharply increased because of the strong reoxidizing effect of the SiO_2 in the slag. This tendency was more significant as the R ratio increased.

The metal-slag reactions in tundish are summarized in the schematic diagram of Figure 11, which is based on the preceding results. The increase in silica activity of molten slag layer, caused by the continuous dissolution of SiO_2 from rice husk powder, exacerbates the reoxidation of molten steel, resulting in the formation of Al_2O_3-rich inclusions. Therefore, the greater the R ratio, the more and the larger alumina inclusions would form in molten steel.

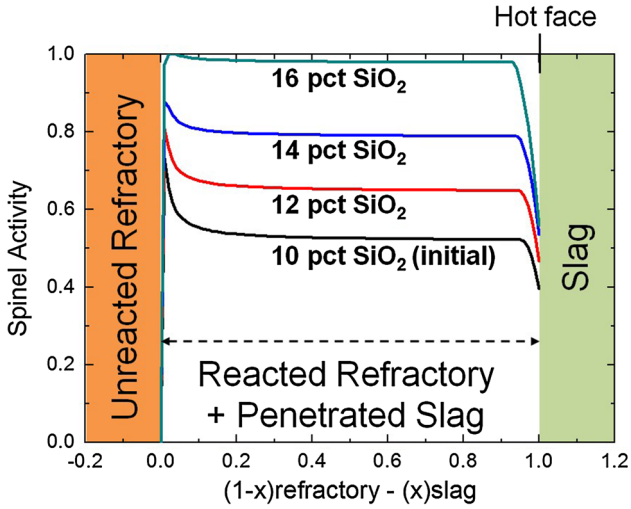

Fig. 14—Activity of spinel compound at the slag-refractory interface at 1823 K (1550 °C).

C. *Corrosion of MgO Refractory by Compositional Changes in Tundish Slag*

The theoretical MgO saturation limit of the molten slag was calculated using FACTSAGE™ 7.0, and the result is shown in Figure 12 as a function of SiO_2 content in the molten slag. It is simply expected that the rice husk (SiO_2 > 85 mass pct) facilitated corrosion of the refractory by dissolution of MgO due to the dramatic increase in its solubility as the SiO_2 was transferred from the rice husk to the molten slag layer.

Backscattered electron images and the element mapping results for the slag-refractory interfacial area are shown in Figure 13 at R ratio = 0.14 and 0.26, respectively. Spinel compound was observed at R ratio = 0.26 (Figure 13(b)), while MgO particles detached from the refractory were observed at R ratio = 0.14 (Figure 13(a)). The activity of spinel compound calculated at the slag-refractory interface is shown in Figure 14 with different SiO_2 contents. The activity of spinel compound increases with increasing content of SiO_2 in the slag, and the spinel compound is precipitated at SiO_2 > 16 mass pct, *viz.* $a_{spinel} = 1.0$. This means that spinel compound is formed more easily at higher R ratio by accelerating the corrosion of MgO refractory.

Sandhage and Yurek investigated the dissolution rate of solid alumina in the CaO-SiO_2-Al_2O_3-MgO slag and concluded that the dissolution of alumina was controlled by the diffusion of Al_2O_3 through the spinel

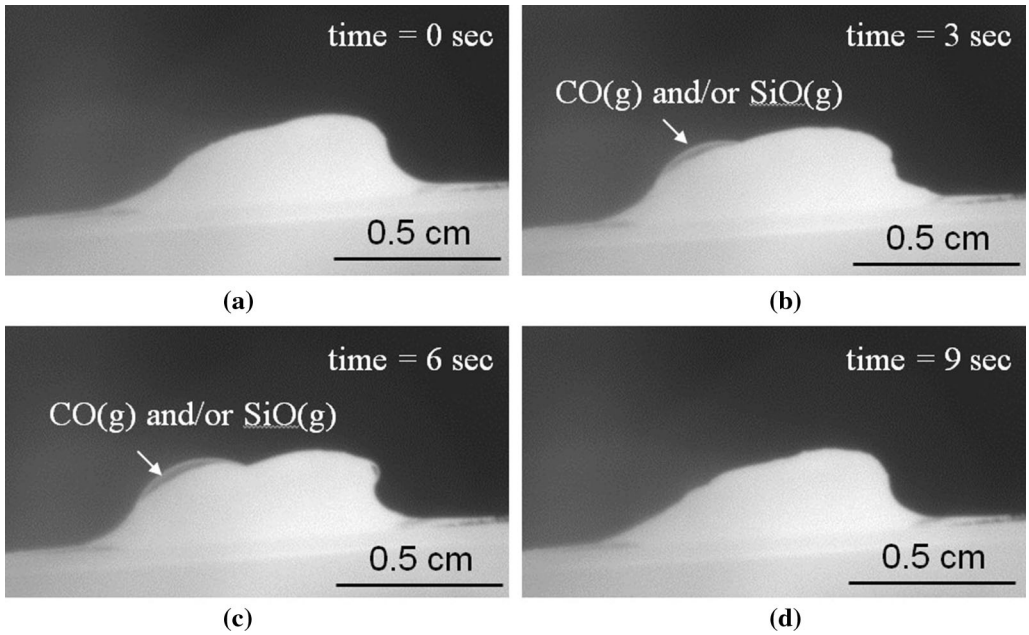

Fig. 15—Evolution of CO or SiO bubbles in the RHA pellet at 1823 K (1550 °C) at (*a*) 0 s, (*b*) 3 s, (*c*) 6 s, and (*d*) 9 s, detected using CCD camera.

layer, which is formed at the vicinity of the interface.[18] Because the formation of the spinel caused indirect dissolution phenomena, the corrosion of alumina was suppressed. Furthermore, Park *et al.*[20] investigated the slag-refractory reaction between $CaO-SiO_2-Al_2O_3-MgO-MnO-CaF_2$ slags and alumina refractory and found the formation of intermediate compound layers, *i.e.*, $CaAl_{12}O_{19}$ and $Mg(Mn)Al_2O_4$ spinel, at the vicinity of the refractory. Furthermore, Chen *et al.*[19] carried out the experiments for the corrosion of MgO refractory immersed into the $CaO-SiO_2-Al_2O_3-MgO-Fe_2O_3$ slags and reported that the formation of spinel layer by slag-refractory reactions, as likely as mentioned previously, retards the corrosion of MgO refractory. However, in the present study, the spinel layer was not observed at the hot face of MgO refractory, as shown in Figure 13. MgO in the refractory directly dissolved into the molten slag layer, which is a completely different situation from the general slag-refractory interfacial reactions investigated by previous researchers.

Filsinger and Bourrie reported that evolution of SiO (g) and CO (g) would occur when SiO_2 is reduced by carbothermic reactions at 1833 K (1560 °C) as follows.[31]

$$SiO_2(s) + C(s) = SiO(g) + CO(g) \qquad [8]$$

In a separate experiment, the evolution of gas bubbles was observed using a CCD camera when the rice husk was heated at 1823 K (1550 °C) under Ar gas (99.9 pct purity), as shown in Figure 15. Because the rice husk contained about 15 mass pct C, as listed in Table I, the gas evolution was anticipated to originate from reaction [8].

Therefore, the evolution of CO or SiO gas bubbles occurred simultaneously in conjunction with the dissolution of SiO_2 at the slag-ash interface. These bubble bursting phenomena probably caused flow motion in the molten slag layer, which resulted in continuous transfer of MgO from the refractory hot face to the bulk slag phase, *viz.* a dilution of MgO possibly occurred near the interface. Hence, it was difficult to form a protective spinel layer at the slag-refractory interface, even though a dissolution of SiO_2 increased the activity of spinel at the interface. Consequently, MgO refractory directly dissolved into the molten slag. A schematic diagram for the reaction mechanism is described in Figure 16. Because the driving force of MgO dissolution increases as the *R* ratio increases, the corrosion of MgO refractory is accelerated by the increase in the *R* ratio. This means that the rice husk insulation powder has a negative effect on the corrosion of MgO refractory during the long casting sequence.

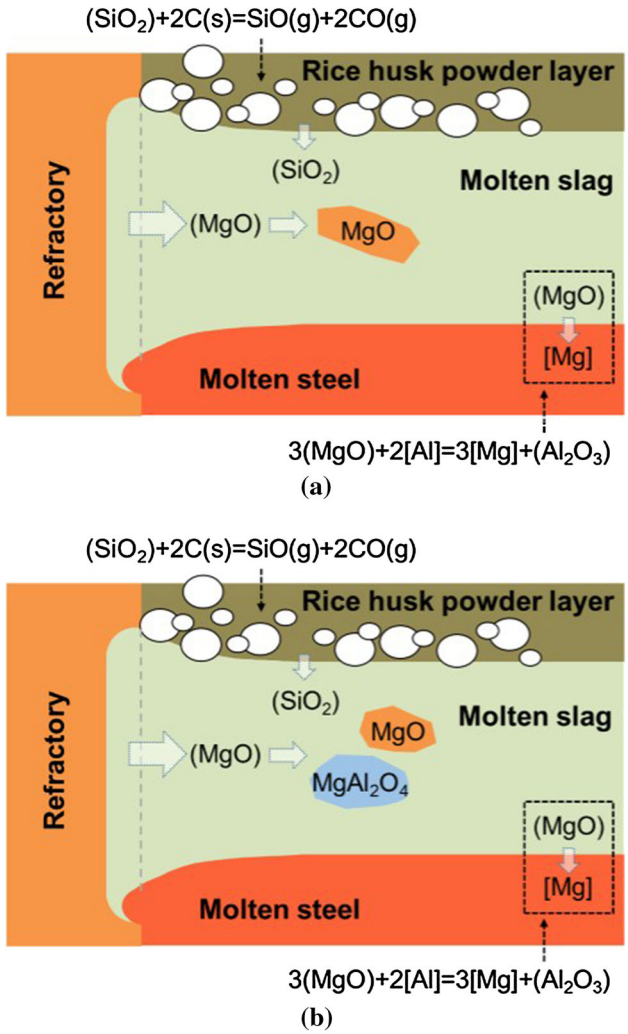

Fig. 16—Schematic diagram of the MgO refractory corrosion at the rice husk-refractory-slag triple junction area with (*a*) *R* ratio = 0.14 and (*b*) *R* ratio > 0.2.

IV. CONCLUSIONS

We investigated how the rice husk, which has been widely used as an insulation powder in steel industry, affects the reoxidation of molten steel in tundish as well as the corrosion of magnesia refractory. The results of this study can be summarized as follows.

1. The oxygen content in the steel remained almost unchanged when a relatively small amount of RHA (*R* ratio = 0.14) was added. However, the oxidation of the steel augmented by increasing RHA (*R* ratio = 0.26 to 1.0), resulting in significant oxygen pickup (ΔO).
2. The reduction rate of SiO_2 from the slag increased with addition of the RHA, while the oxidation rate of Al in the steel was not critically dependent on the *R* ratio. The rate-determining step of the reoxidation reaction of Al was stated to be the mass transfer of Al in the liquid metal phase.
3. The increase of the silica activity in the slag layer by increasing the *R* ratio promoted the self-dissociation of SiO_2 from the slag layer into the molten steel (*i.e.*, $SiO_2 = Si + 2O$), which caused silicon and oxygen pickup as the *R* ratio increased.
4. The total number of inclusions formed *via* reoxidation in the steel dramatically increased per unit area by increasing the *R* ratio, which was consistent with the results of initial oxygen pickup tendency.

Moreover, the relative population and average size of Al_2O_3-rich inclusions increased by increasing the R ratio.

5. The MgO in the refractory directly dissolved into the molten slag layer without forming any intermediate compound layer, *e.g.*, spinel, which is a completely different situation from the general slag-refractory interfacial reaction. Possibly flow was induced by the bursting of gas (CO or SiO) bubbles at the ash-slag (-refractory) interface, since the silica was reduced by solid carbon in the RHA.

REFERENCES

1. N. Bessho, H. Yamasaki, Y. Fuji, Y. Nozaki, and S. Hiwasa: *ISIJ Int*., 1992, vol. 32, pp. 157–63.
2. Y. Habu, H. Kitaoka, Y. Yoshii, T. Emi, Y. Iida, and N. Ueda: *Tetsu-to-Hagané*, 1976, vol. 62, pp. 1803–12.
3. H. Tanaka, R. Nishihara, R. Miura, R. Tsujino, T. Kimura, T. Nishi, and T. Imoto: *ISIJ Int*., 1994, vol. 34, pp. 868–75.
4. K. Sasai and Y. Mizukami: *ISIJ Int*., 2000, vol. 40, pp. 40–47.
5. H. Tanaka, R. Saibara, R. Hara, I. Kitagawa, and R. Tsujino: *Tetsu-to-Hagané*, 1993, vol. 79, pp. 1254–59.
6. L. Kuchar and L. Holappa: *Proc. 76th Steelmaking Conf*., 1993, pp. 28–31.
7. L. Holappa, S. Nurmi, and S. Louhenkilpi: *Rev. Metal*., 2009, vol. 106, pp. 9–20.
8. V. Manninen, T. Lano, and L. Holappa: *Scand. J. Metall*., 2000, vol. 29, pp. 156–65.
9. Y. Higuchi, Y. Tago, S. Fukagawa, T. Kanai, and A. Mutoh: *Tetsu-to-Hagané*, 1999, vol. 85, pp. 375–81.
10. Y. Sahai and T. Emi: *Tundish Technology for Clean Steel Production*, World Scientific, Singapore, 2008, pp. 201–02.
11. H. Sun and K. Mori: *ISIJ Int*., 1996, vol. 36, pp. S34–37.
12. M.A. Rhamdhani, G.A. Brooks, and K.S. Coley: *Metall. Mater. Trans. B*, 2005, vol. 36B, pp. 219–27.
13. Y.B. Kang, M.S. Kim, S.W. Lee, J.W. Lee, J.W. Cho, M.S. Park, and H.G. Lee: *Metall. Mater. Trans. B*, 2013, vol. 44B, pp. 309–16.
14. J. Park, S. Sridhar, and R.J. Fruehan: *Metall. Mater. Trans. B*, 2014, vol. 45B, pp. 1380–88.
15. D.C. Park, I.H. Jung, Peter.C.H. Rhee, and H.G. Lee: *ISIJ Int*., 2004, vol. 44, pp. 1669–78.
16. Y. Chung: Ph.D. Thesis, Carnegie Mellon University, Pittsburgh, PA, 1999.
17. T. Tanaka, H. Goto, M. Nakamoto, M. Suzuki, M. Hanao, M. Zeze, H. Tamamura, and T. Yoshikawa: *ISIJ Int*., 2016, vol. 56, pp. 944–52.
18. K.H. Sandhage and G.J. Yurek: *J. Am. Ceram. Soc*., 1990, vol. 73, pp. 3643–49.
19. Y. Chen, G.A. Brooks, and S.A. Nightingale: *Can. Metall. Q*., 2005, vol. 44, pp. 323–29.
20. J.S. Park, D.H. Kim, and J.H. Park: *J. Am. Ceram. Soc*., 2015, vol. 98, pp. 1974–81.
21. J.S. Park and J.H. Park: *Metall. Mater. Trans. B*, 2016, vol. 47B, pp. 3225–30.
22. S. Feichtinger, S.K. Michelic, Y.B. Kang, and C. Bernhard: *J. Am. Ceram. Soc*., 2014, vol. 97, pp. 316–25.
23. T.S. Kim and J.H. Park: *ISIJ Int*., 2014, vol. 54, pp. 2031–38.
24. D.J. Kim and J.H. Park: *Metall. Mater. Trans. B*, 2012, vol. 43B, pp. 875–86.
25. S.K. Kwon, Y.M. Kong, and J.H. Park: *Met. Mater. Int*., 2014, vol. 20, pp. 959–66.
26. J.S. Park and J.H. Park: *Steel Res. Int*., 2014, vol. 85, pp. 1303–09.
27. S.K. Kwon, J.S. Park, and J.H. Park: *ISIJ Int*., 2015, vol. 55, pp. 2589–96.
28. Y.S. Han, D.R. Swinbourne, and J.H. Park: *Metall. Mater. Trans. B*, 2015, vol. 46B, pp. 2449–57.
29. Y.S. Han and J.H. Park: *Metall. Mater. Trans. B*, 2015, vol. 46B, pp. 235–42.
30. J.H. Park and H. Todoroki: *ISIJ Int*., 2010, vol. 50, pp. 1333–46.
31. D.H. Filsinger and D.B. Bourrie: *J. Am. Ceram. Soc*., 1990, vol. 73, pp. 1726–32.